DOE/NV/10872--T179

QUARTERLY REPORT

TO

US DOE YMSCO

FROM

HEAT TRANSFER LABORATORY
MECHANICAL ENGINEERING DEPARTMENT
UNIVERSITY OF NEVADA, LAS VEGAS

"HEAT TRANSFER STUDIES"

R. BOEHM, PI
Y.-T. CHEN, CO-PI
L. MA

APRIL 20, 1995

Abstract

Nitrogen gas has been replaced by room air in the extension of multi-phase models to sub-residual saturation experiments on drying. The TOUGH2 code has been used to simulate the same problem with the identical boundary conditions.

A constant heat flux boundary condition on the heater has been performed in the repository drift experiment. The desired constant heat flux can produce a steady-state heater temperature (≈ 238°C) close to the constant heater surface temperature used before. What occurs in the air annulus and in the porous medium with the different thermal boundary conditions and water quantities is reported.

Table of Contents

A Study of the Extension of Multi-Phase Models to Sub-Residual Saturation

This study is focusing on the limitations of applying multi-phase flow models to the hydrothermal processes occurring when the liquid saturation falls below residual levels. Multi-phase transport in geological media at sub-residual saturations is of considerable importance in various applications including performance studies of the high-level radioactive waste repository, decontamination of hazardous waste sites, wood drying processes, and several other drying applications. The majority of the work performed in hydrogeologic modeling has been confined to isothermal studies and/or at liquid saturations well above residual levels. Recently, the problem of contaminant transport in the sub-residual regime has attracted considerable attention, particularly when dealing with the disposal of high-level radioactive waste in an underground repository. As a consequence, it is of importance to understand the drying effects of residual water in porous media. The capillary pressure within the porous medium is a function of thermal gradients present.

An experimental program in our laboratory continues to study the drying effects of residue water in porous media. A flow of air through a porous medium is used to determine from experimental measurements the physical relationship between the liquid saturation, capillary pressure, and temperature. In one set of experiments a low flow rate of air with an isothermal boundary condition has been used, and in another set, a high flow rate of the same air with an adiabatic boundary condition will be applied. These results may give useful information for numerical modelers. To furnish data to support numerical modelers in evaluating their results is the main task of this experiment. As a step in this direction, the TOUGH2 code is being used to simulate the same problem with the identical boundary conditions. Results will be compared from the calculations and the experiment.

The new experimental setup is shown in Figure 1. The details of the redesigned test section is shown in Figure 2.

As currently conceived, the test section has been reconstructed of a 16" long aluminum cylinder that has an inside diameter of 1.5" and two windows (0.275" x 5.625"). The reason why aluminum was chosen for this applications is because it is rust resistant and it has a high thermal conductivity. A constant heat flux or temperature boundary condition can be applied on the outside of the aluminum wall.

Room air is used as the displacing fluid and water is the displaced fluid in the glass beads. Several different mass flow rates of air with heating effect will be added

to the experimental study. The mass flow rate of air is controlled by a vacuum and a buffer tank system. The very low mass flow rate of air is calculated using a soap bubble volumetric instrument and U-tube manometer. Tests begin at the residual saturation condition and continue until steady-state conditions are reached, which may or may not find a completely dried porous medium.

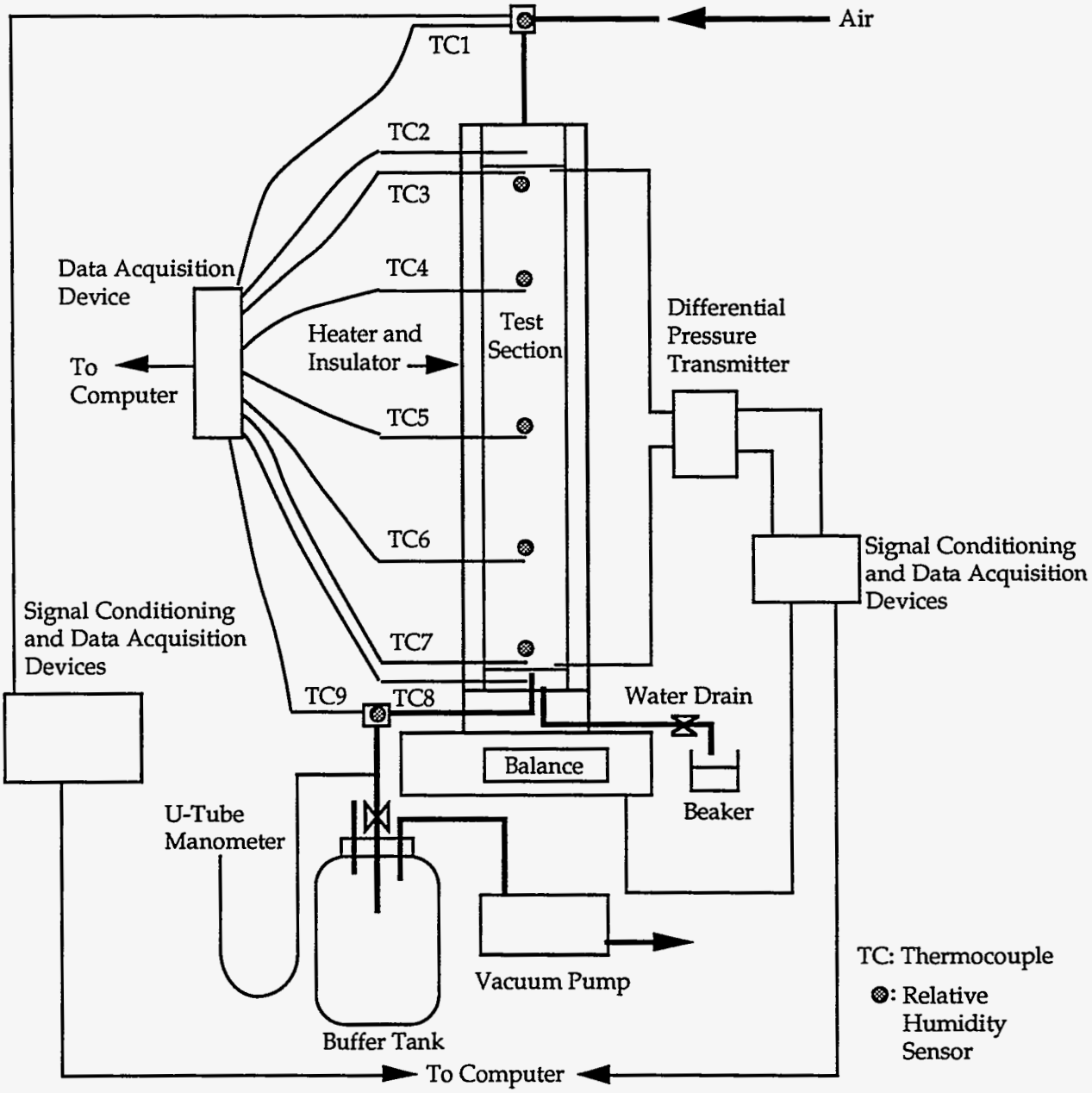

Figure 1. Diagram of piping and instrumentation used in the drying experiment.

Two new commercial relative humidity sensors, the product of the Phys-Chem Scientific Corp., are used to measure the inlet and outlet water moisture content of the air. These sensors have about ± 1% accuracy, based on the full range measurement. The operating relative humidity range is from 0 to 100%. The operating temperature range is -40 to 100°C. These sensors have a 10 sec response for a step change from 11% RH to 93%. The average temperature coefficient is about -0.3% RH/°C. The sensor size is 0.30" x 0.50"x 0.025", and it has SIP connections with 0.10" mounting centers. Calibration of the humidity sensors as a function of water content and temperature is done following the appropriate ASTM method. During the tests, the output of the humidity sensors are recorded as a function of time.

Most of the instrumentation used has been described in earlier reports. In the current tests, a small-range differential pressure transmitter replaces a larger-range one for measuring the pressure drop across the porous medium. The output voltages from the transmitter are also recorded as function of time. A Setra Model 264 differential pressure transmitter (0.25" water maximum range) has been purchased. It demonstrates an accuracy better than ± 1% of full scale.

0.037" diameter (average) glass beads are used as the fill material in the test section. The glass beads are cleaned using a 1% hydrochloride solution and distilled water. Weight readings of the entire test section with respect to time are also recorded during the test, and these are accomplished with a digital balance with an electrical signal output. A digital balance of 4 kilogram capacity, a 0.1 gram readability, and ±1% accuracy is used to measure the weight of test section. Comparisons can be made between the change of water content in the test section inferred from the mass flow of water out (estimated from the air mass flow and humidity measurements) with readings taken from the digital balance.

Nine 30 gauge K-type thermocouples are used in the test section to measure the temperatures with a maximum of 0.75% error. These are placed at several locations within the test section as well as in the inlet and outlet humidity sensor boxes.

Room temperature and atmospheric pressure are measured. A computer with a LabVIEW data acquisition system is used to collect all data from the experiment.

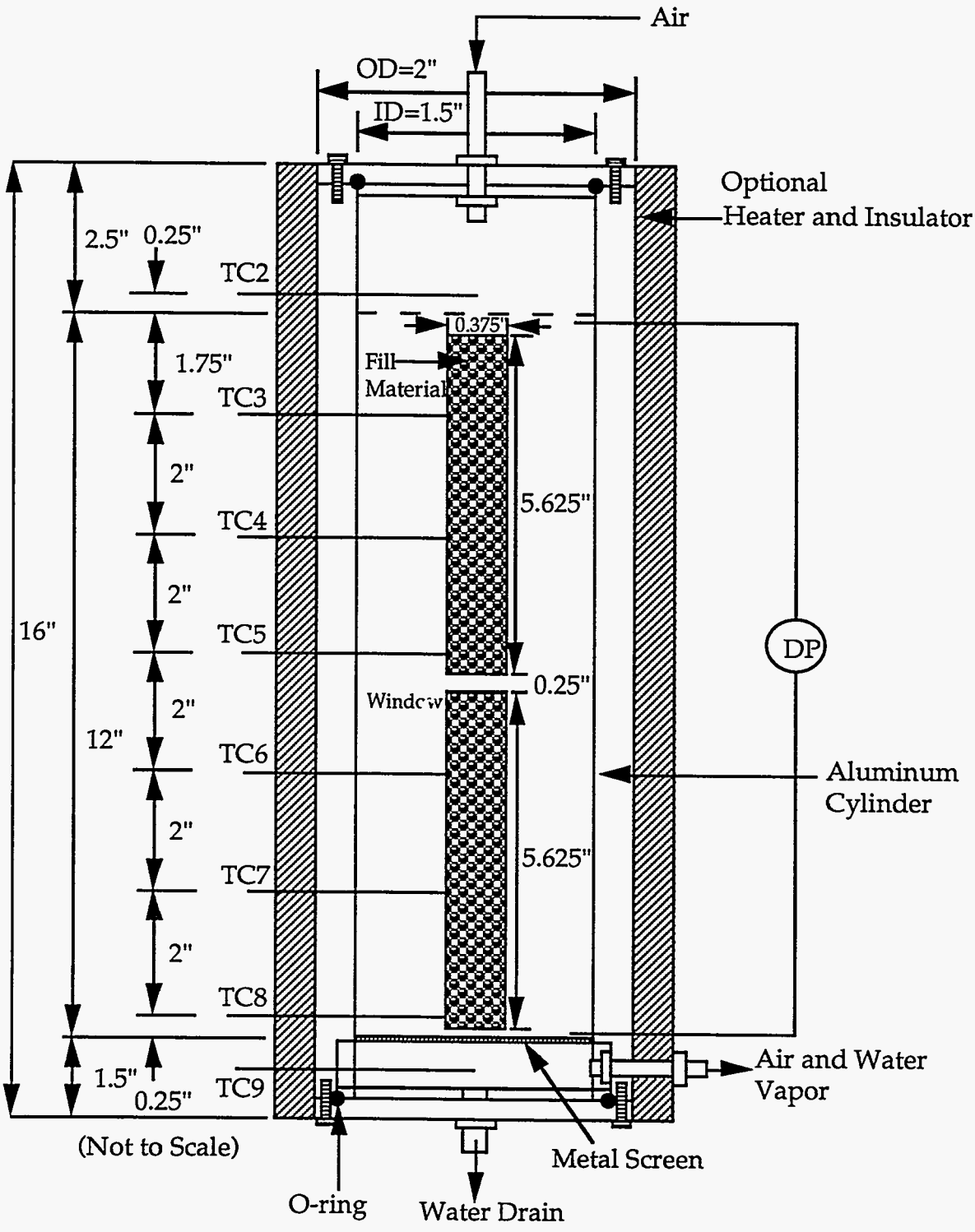

Figure 2. Schematic diagram of the test section used in the drying experiments. Two windows on one side allow visual observations during the test runs. The test section can be operated with or without heating.

A Study of Unsaturated Flows with Heat Transfer in the Repository Drift

The experimental design described in the previous report has been used to investigate the water flow through a rigid porous medium with heat transfer around a non-backfilled hole. Figure 3 shows a rigid porous medium approximately 1.5" x 12" x 12" (high) that was prepared with a 1.5" hole through the thin dimension of the medium. A 1" diameter, 1.5" long 500 W electrical cartridge heater was installed horizontally through the medium, forming an air annulus in the hole. A ceramic insert was used to seal both sides of the air annulus and to support the heater in the air annulus.

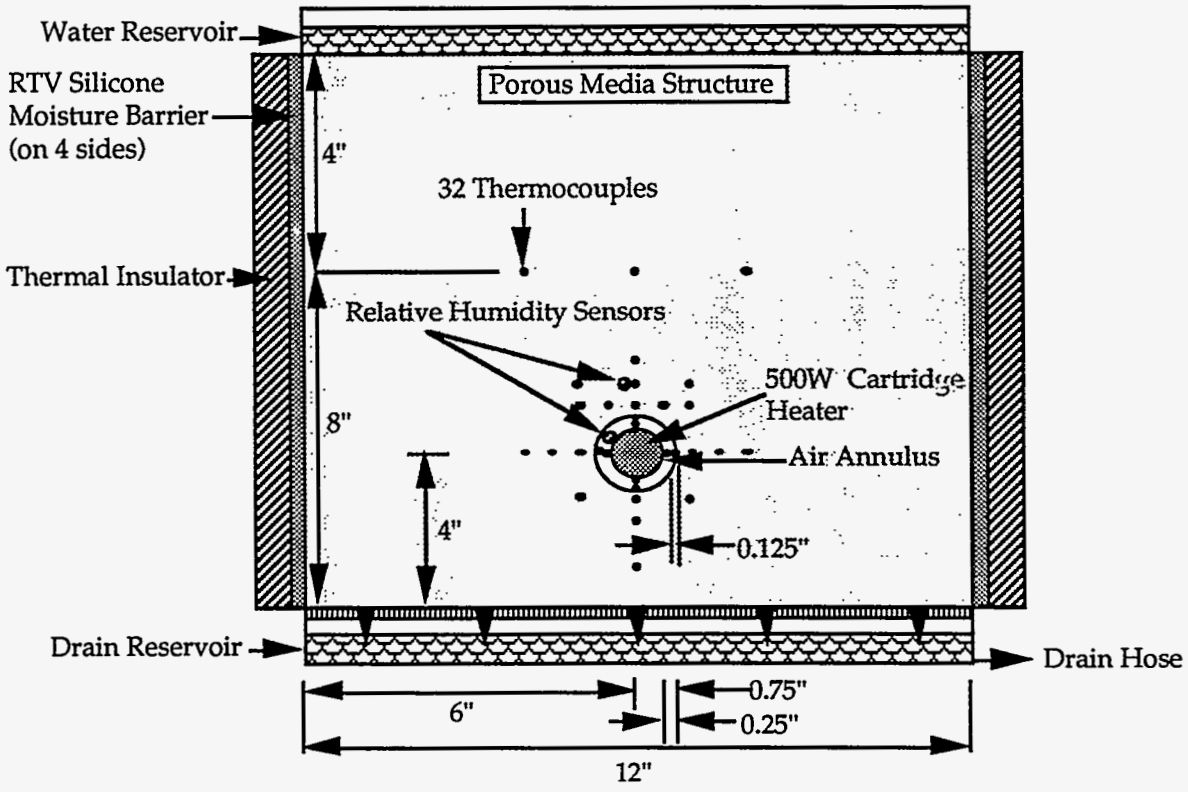

Figure 3. A front-view schematic of the experimental setup to simulate some aspects of flows around an underground repository. The dimension into the page is 1.5 in.

Thermocouples are inserted into the medium from the large surface side. Nine and twenty-three 30 gauge K-type thermocouples are used to measure the temperatures in the air annulus and the porous medium structure, respectively. Two capacitance humidity sensors are used to measure the humidities in the porous medium and in the air annulus. The configuration of thermocouples in the porous medium is shown in Figure 4. The sides of the porous medium are sealed so that

moisture cannot escape through those surfaces. The permeability of the porous media structure is about 5.54×10^{-11} ft^2. Of particular concern is the determination of the temperatures near and in the annulus, and the humidity in the annulus. Data are logged every 10 seconds on a personal computer using LabVIEW software and hardware.

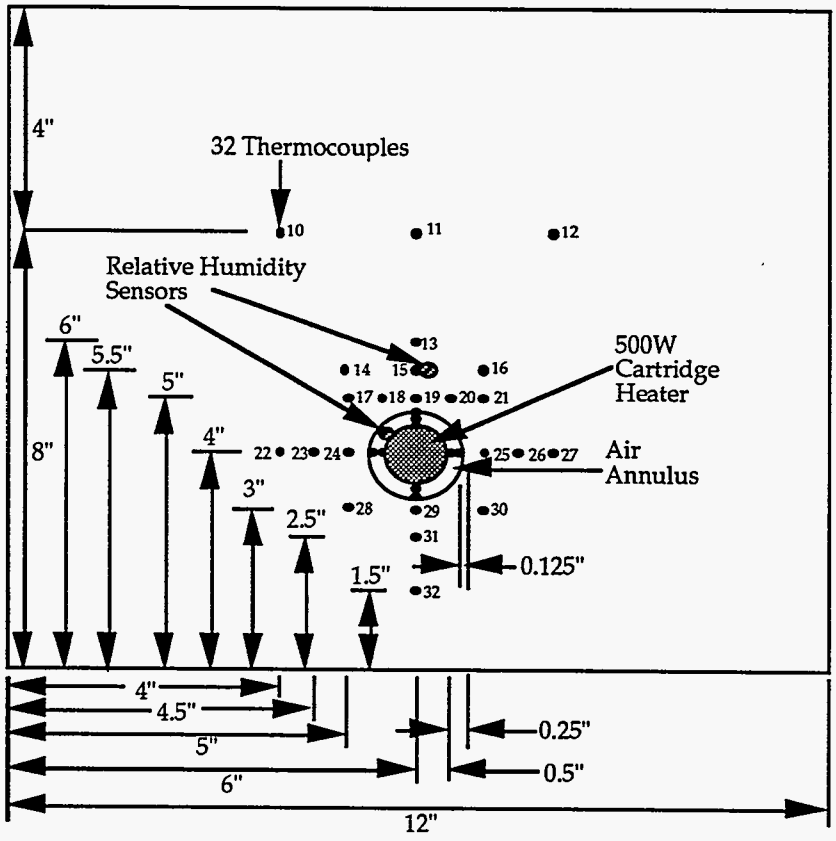

Figure 4. Schematic location of the thermocouples and humidity sensors in the repository flow experiments.

An experimental run begins with a dry porous material and the constant heat flux (i.e. 20.2 V and 0.64 A) on the heater dissipating the necessary power to achieve a specific temperature. In this report, studies of a constant heat flux condition is reported that yields a high heater temperature (≈ 238°C) at the dry condition. Tap water at ambient temperature is introduced from the top of the porous medium when a steady state dry condition in the porous medium and air annulus is reached. With constant heat flux conditions, the heater temperature does not remain constant when water and/or vapor penetrates into the air annulus.

The particular focus of the work reported here is the comparison of two different thermal boundaries on the heater. The constant surface temperature of

heater and the constant heat flux from the heater have been studied. Experiments was performed using 200 ml water being poured onto the top of the 12" x 1.5" surface. The effect of water quantity on the response of the constant heat flux system will be investigated later.

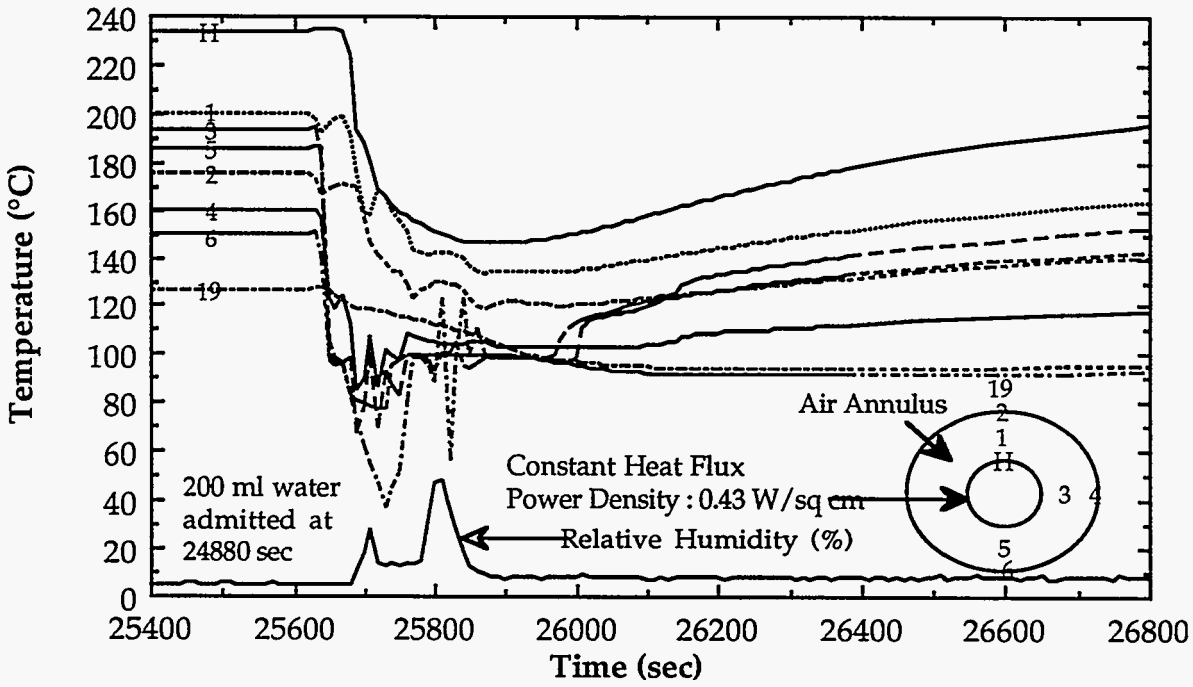

Figure 5. Variations of temperature and relative humidity in the air annulus with a constant heat flux and 200 ml of water flowing through the system.

Figure 5 shows the variations of temperature and relative humidity in the air annulus with a constant heat flux from the heater with a small (200 ml) quantity of water. The temperatures in the air annulus and on the wall of annulus have different responses when moisture reaches those points. Heater temperature decreases from 237°C to 145°C while moisture stays in the air annulus. It increases gradually back to the steady-state condition when the drying process starts. Thermocouples 1 and 2 indicate that the temperatures are higher than the water boiling point when moisture reaches there. Thermocouples 3 and 4 show a small fluctuation when moisture reaches there and indicate temperatures decrease to a saturated steam temperature value. Thermocouples 5 and 6 show a big fluctuation and thermocouple 6 indicates an overcooling phenomena at the bottom wall of the air annulus. This may indicate that steam condensation occurs on the bottom wall. The relative humidity in the air annulus shows two peaks that indicate a 25%

increase at the first peak and a 43% increase at the second peak when steam penetrates the air annulus. The reason why the relative humidity has two peaks may be that subcooled condensation occurs in the air annulus. The thermal resistance to the moisture is no longer strong enough to keep moisture away from the air annulus. The system needs about an hour to return to steady state at approximately the same temperature as existed before water admission. The water boiling point is about 98.1°C, and this is calculated from the atmospheric pressure during the test. Details of the responses of thermocouples 5 and 6 are shown in Figure 6.

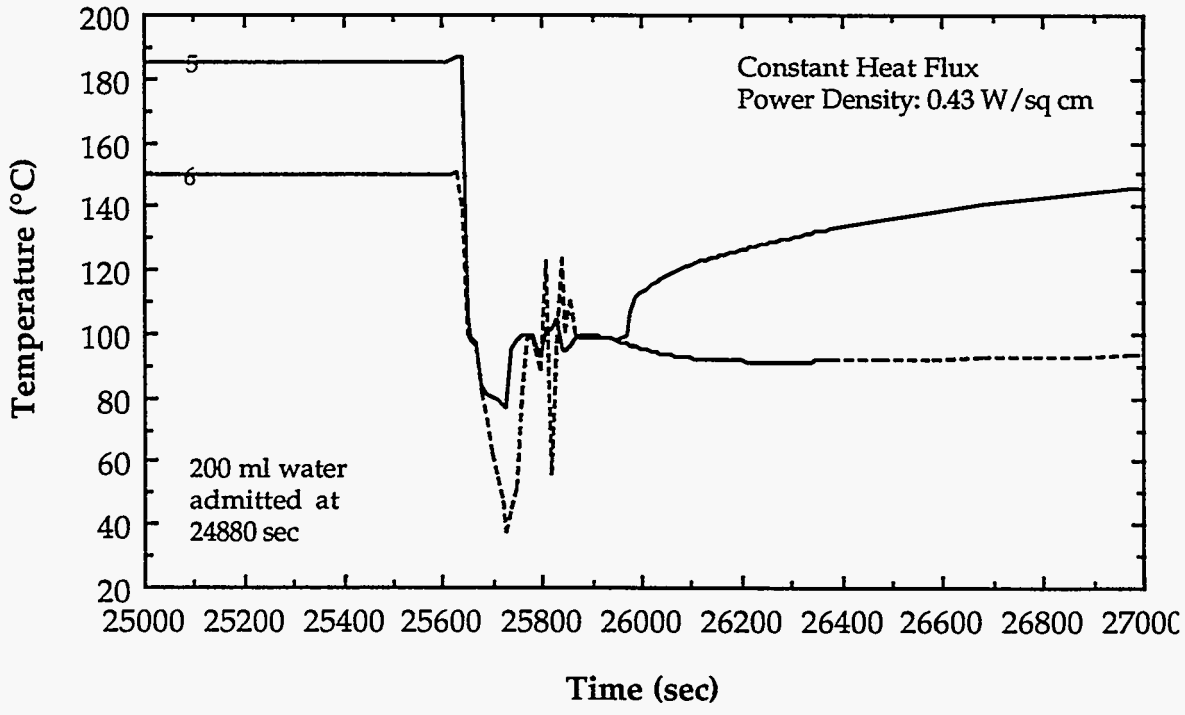

Figure 6. Variations of temperature at thermocouples 5 and 6 in the air annulus with a constant heat flux and 200 ml of water flowed through.

Figure 7 shows variations of temperature at a 5 in height within the porous medium, which is 0.25 in above the rim of air annulus, when a constant heat flux and 200 ml water is present. The temperatures dropped from above the water boiling point, which was 98.1°C during these tests, to a mixture of water vapor and liquid temperatures when moisture reached these points. The locations of thermocouples 17 and 21 showed a water vapor and liquid retention for about one and half hour before those locations dried out. Thermocouples 19 and 20 show a

97°C and 95°C decrease when water flowed through, respectively. A phase change apparently occurred at the locations of thermocouples 17, 18, 19, 20, and 21. A mixed heat transfer mechanism of convection and conduction could be substantiated.

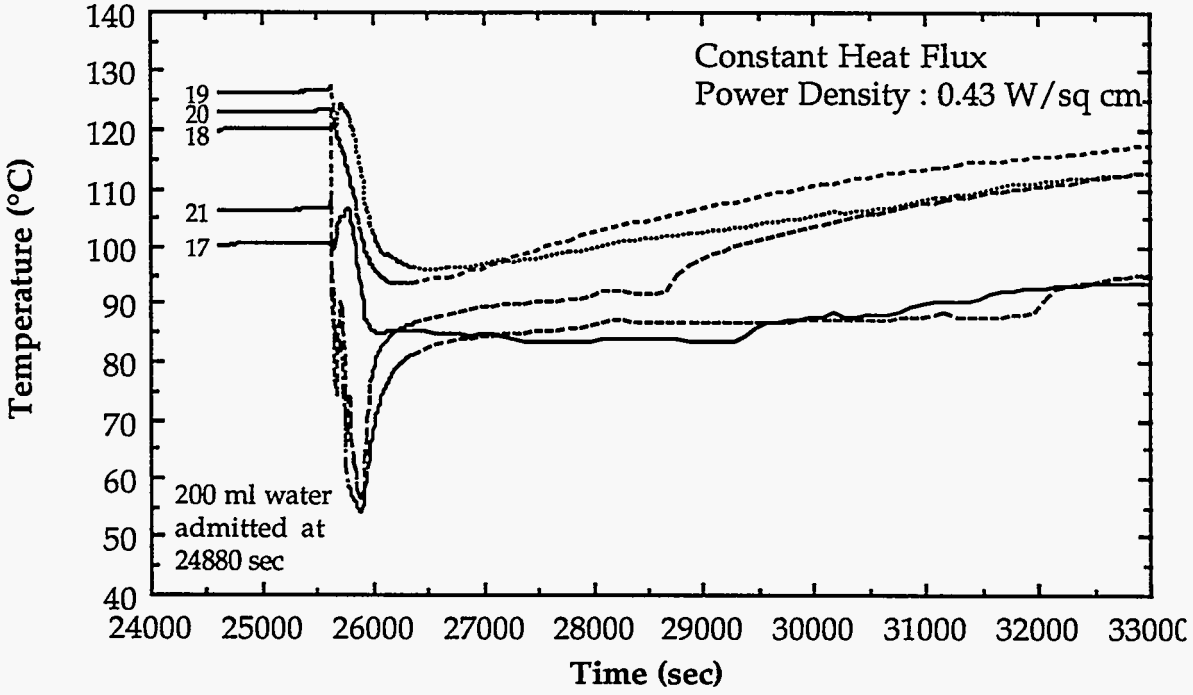

Figure 7. Variations of temperature at a 5" height in the porous medium with a constant heat flux and 200 ml quantity of water.

Figures 8 shows variations of temperature at a 5.5 in height in the porous medium with a constant heat flux and 200 ml of water. Thermocouple 15 shows a 56°C decrease when cool water is admitted from the top. It remained at 88°C for about 45 minutes, which apparently shows that hot water is present during this time. This temperature then increases slowly back above the water boiling point. Thermocouples 14 and 16 show saturated steam and water were apparently there for a few minutes when water vapor reaches those points. Both thermocouples showed an increase in temperature followed by a cooling phenomenon. This latter effect, where the thermocouples showed a drop of about 40°C and 32°C, respectively, probably indicates that some evaporation occurred. A significant refluxing phenomena occurs in these regions. Thermocouples 14, 15, and 16 decrease when the cool water flowed through those points and increase when the water vapor is present. It is an important to note that this observation agrees with the effects of the high heater temperature with the 200 ml water experiment.

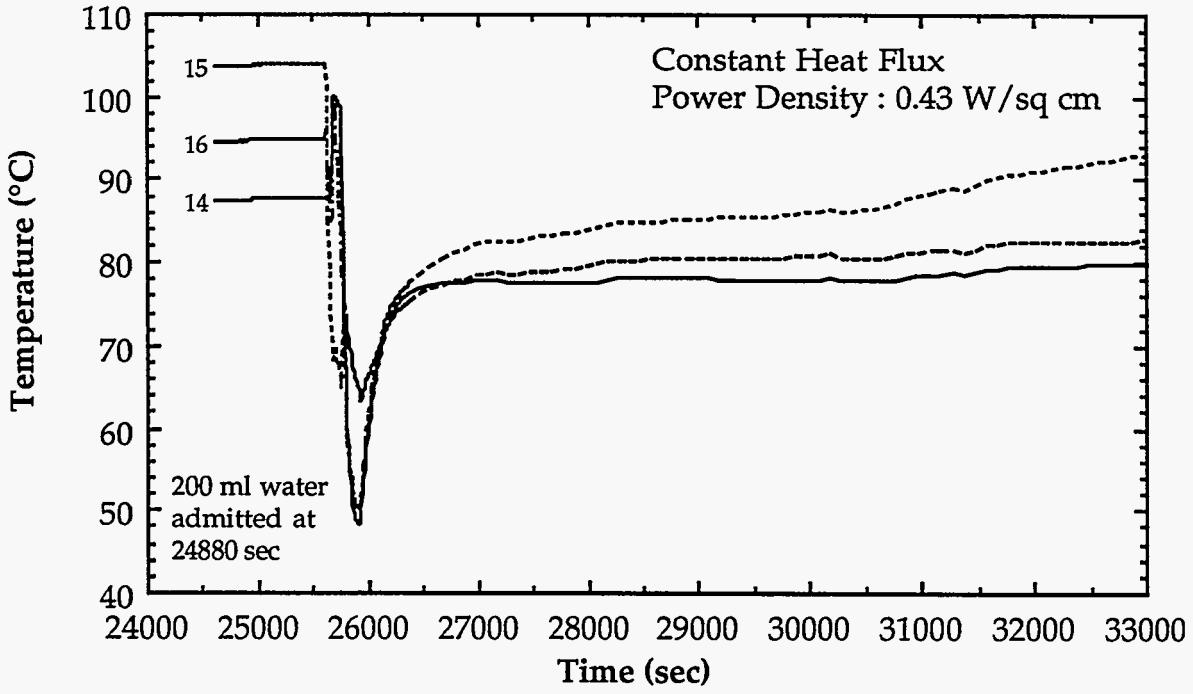

Figure 8. Variations of temperature at a 5.5" height in the porous medium with a constant heat flux and 200 ml quantity of water.

Figure 9 shows variations of temperature at the left hand side of the air annulus with a constant heat flux and 200 ml water. Thermocouple 24 is located in the porous medium 0.25 in to the left of the rim of the air annulus. Its temperature remains at a constant value which is above the water boiling point before water admission from the top of porous medium. When water flows through this point, the region around thermocouple 24 contains saturated steam and water. This region then dries out and temperatures return back to their steady state values. Thermocouple 23 shows a contrasting behavior to this. Readings from thermocouple 23 remained at a constant value which is below the water boiling point before the water vapor reached this point. The reason why the temperature did not drop first when the water flowed through this point could also be explained by a heating effect from the top of the porous medium to that point. A detailed check of recorded temperature data showed that steam above the boiling point was present for about 5.5 minutes around this thermocouple. This was apparently followed by some liquid being evaporated, and this caused the temperature to decrease. The net result yielded a temperature about 14°C below the steady state temperature. It can be inferred from the two major peaks present that significant

refluxing phenomena occurred within the next 1.7 hours. A complicated heat transfer mechanism of conduction and convection probably took place, but the convection heat transfer dominates in the refluxing region. Thermocouple 22 has a similar response to that shown for thermocouple 23 but without an significant indication of refluxing being present. Continuous phase change phenomena may be taking place here. The right and left hand sides of the air annulus show symmetrical temperature responses.

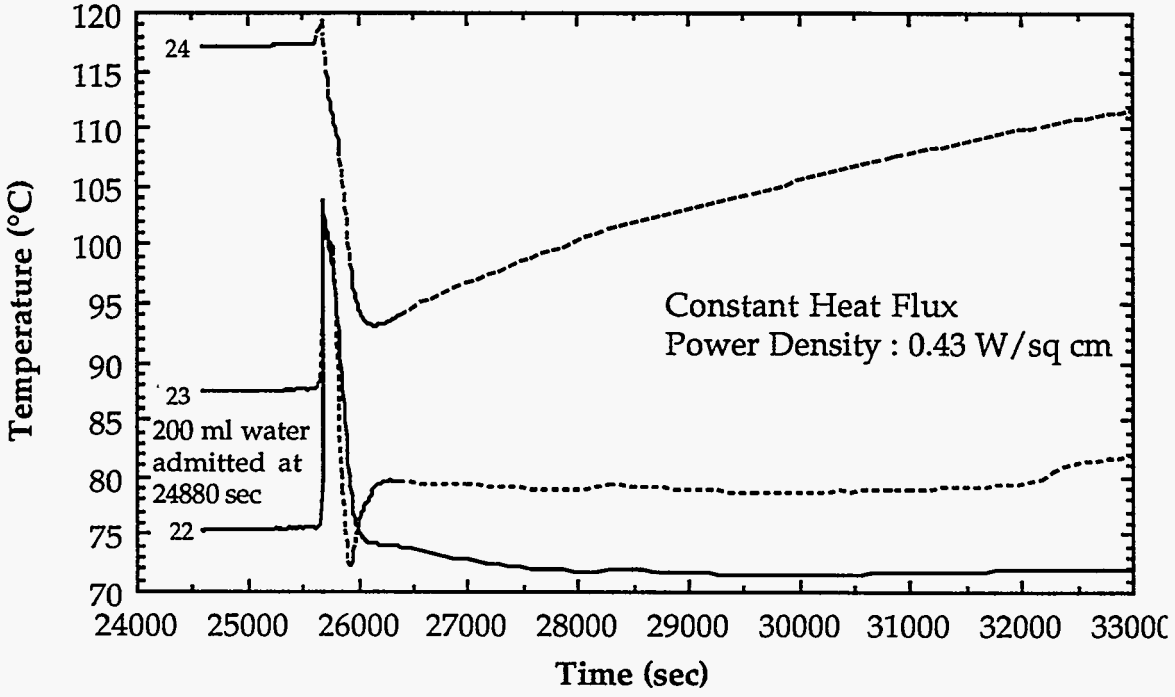

Figure 9. Variations of temperature at the left hand side of air annulus with a constant heat flux and 200 ml quantity of water.

Figure 10 shows variations of temperature at a 3 in height in the porous medium with a constant heat flux with 200 ml water. Thermocouple 29 shows that this location in the porous medium remains at the boiling point (saturated steam is probably present) for a very short time and then a cooling effect occurs at this point when the low temperature moisture reaches there. It is of interest to note the response of thermocouple 29. It starts to increase drastically after an hour retention. Thermocouples 28 and 30 also indicate that the boiling point is reached. The fluid is apparently heated up when it travels through and around the air annulus. Thus, it causes a small heating effect in the regions of thermocouples 28 and 30.

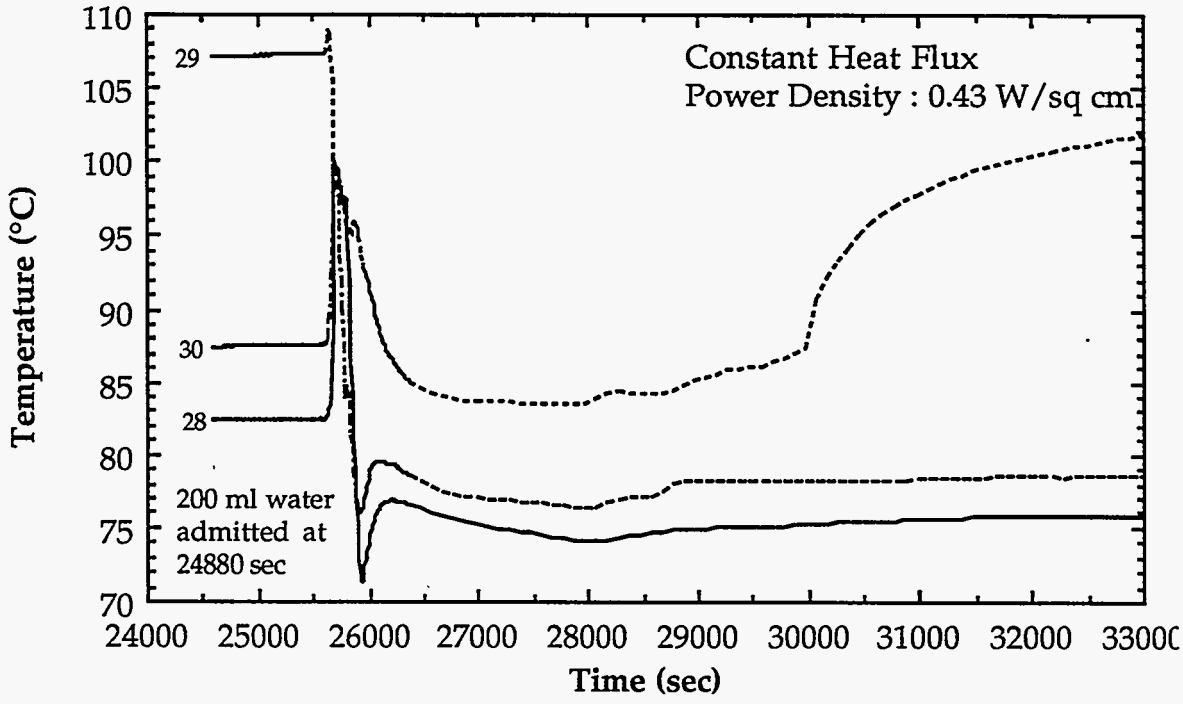

Figure 10. Variations of temperature at a 3" height in the porous medium with a constant heat flux and 200 ml quantity of water.

Thermocouples 10, 11, and 12 all demonstrate the same kinds of responses due to fluid cooling effects on these regions. Figure 11 shows variations of temperature at a 8 in height in the porous medium for the constant heat flux with 200 ml water.

Figure 12 shows the variations of temperature at a vertical top in the porous medium with a constant heat flux and 200 ml water. Figure 13 shows the variations of temperature at a vertical bottom in the porous medium with a constant heat flux and 200 ml water. Figure 13 shows variations of temperature in a vertical line directly below the center of the annulus. Thermocouple 31 in Figure 13 indicates that location reaches the boiling point for a short period of time. The temperature then slowly decreases as the medium dries. A similar response, but lower in temperature overall, is shown for thermocouple 32.

Figure 14 shows the relative humidity at air annulus and thermocouple 15 with a constant heat flux and 200 ml water vs. time. Between 32900 and 33800 seconds there are few disturbances shown on the relative humidity curve and this is followed by a 14% increase and then drops back to the steady state value.

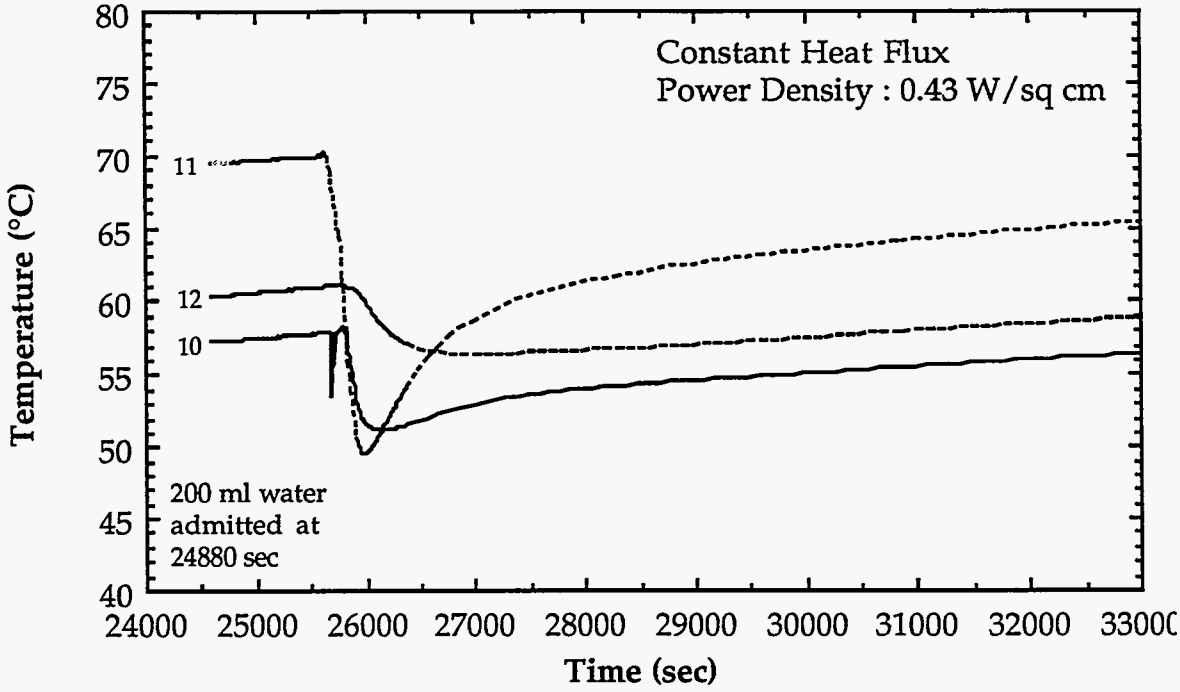

Figure 11. Variations of temperature at a 8" height in the porous medium with a constant heat flux and 200 ml quantity of water.

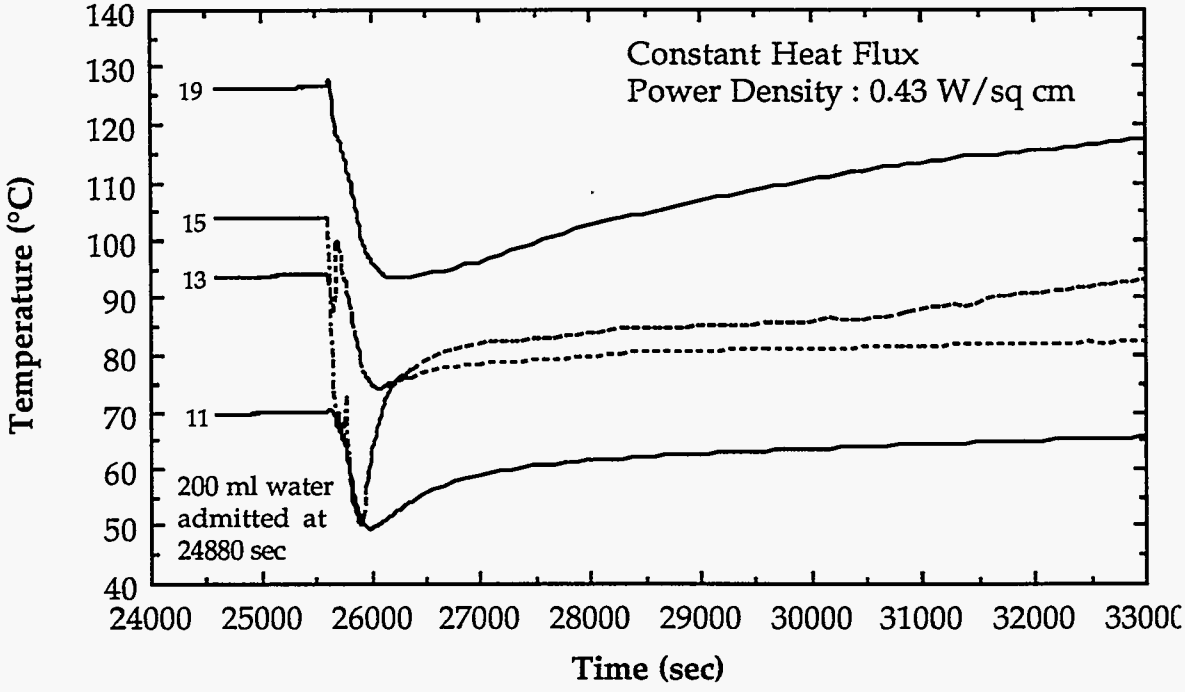

Figure 12. Variations of temperature at a vertical top the porous medium with a constant heat flux and 200 ml quantity of water.

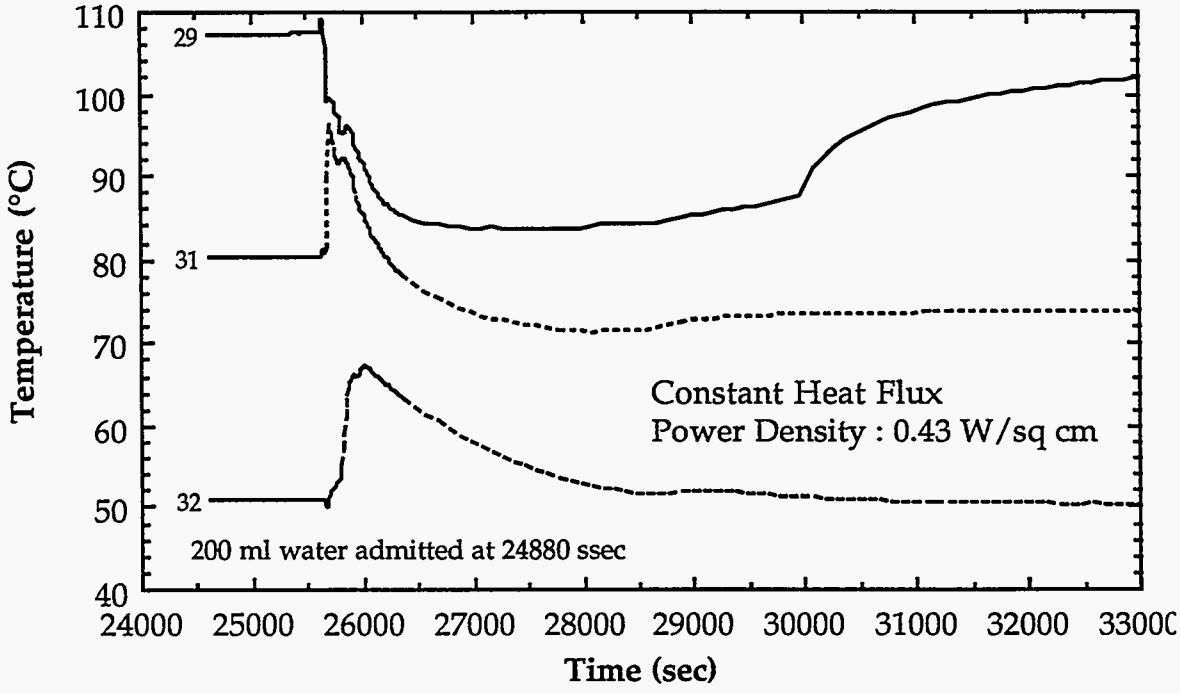

Figure 13. Variations of temperature at a vertical bottom the porous medium with a constant heat flux and 200 ml quantity of water.

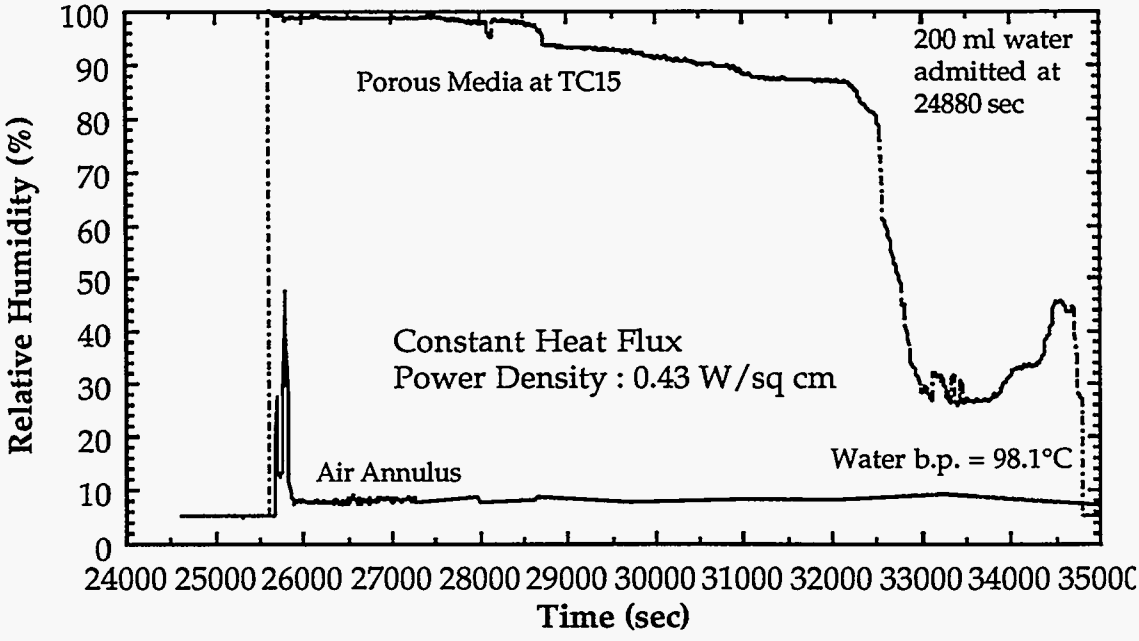

Figure 14. Relative humidity at air annulus and thermocouple 15 with a constant heat flux and 200 ml quantity of water.

Figures 15, 16, 17, 18, 19, and 20 show the comparison of temperature in the air annulus with the different thermal boundaries on the heater and water quantities from the top of porous medium. The results are apparently consistent. It is not difficult to find the constant heat flux boundary condition on the heater will prolong the time for returning the temperatures back to steady-state. This is because the heater temperature has a similar profile after water penetrated into the air annulus. Figure 15 shows the air temperatures in the annulus above the heater. It can be noted that the temperature decrease is less for the constant heater surface temperature (238°C) case than the constant heat flux case after moisture reaches that point, with the same water quantity. Figure 16 shows the top wall temperatures in the air annulus. They have a very similar temperature drop for both the constant surface heater temperature (238°C) and the constant heat flux with the same water quantity. Figure 17 shows the air temperatures in the annulus on the side of the heater. Less temperature decrease is seen for the constant heater surface temperature (238°C) case than for the constant heat flux situation. Figures 18 and 19 show the side wall and bottom air temperatures in the air annulus, respectively. Figure 20 shows the bottom wall temperatures in the air annulus. At the constant heat flux boundary condition, retention time is longer than the constant heater surface temperature.

Figures 21, 22, 23, 24, 25, 26, 27, 28, and 29 show the comparison of temperature in the porous medium for the different thermal conditions and water quantities. Figure 21 shows the temperatures from thermocouple 19. The constant heater surface temperature boundary condition and the constant heat flux boundary condition have a similar temperature response. The only difference is the constant heat flux boundary condition needs a longer time to return back to steady-state. Figures 22 and 23 show the temperatures from the thermocouples 17 and 18, respectively. Figure 22 shows a similar temperature drop for the two thermal boundary conditions and a longer drying time for the constant heat flux boundary condition. Figure 24 shows the temperatures from thermocouple 22. Figure 25 shows the temperatures from thermocouple 23. The refluxing phenomena can be found for both thermal boundary conditions. Figures 26, 27, 28, and 29 show the temperatures from thermocouples 24, 28, 29, and 31, respectively. The temperature responses are very consistent for the different thermal boundary conditions.

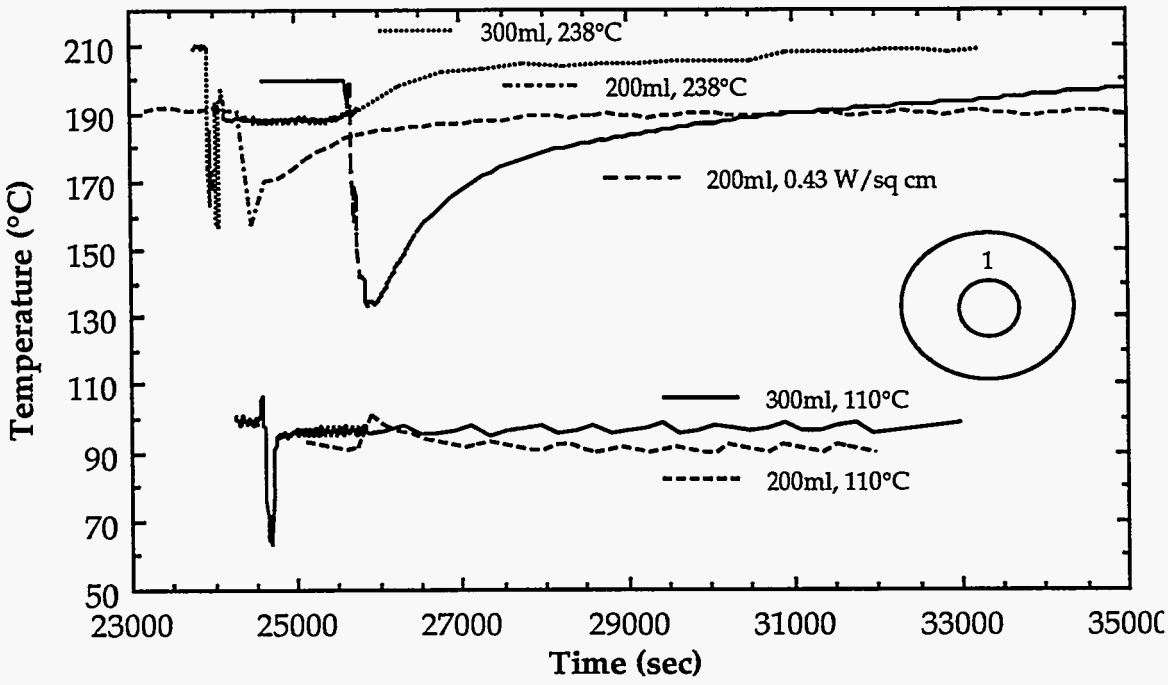

Figure 15. Comparisons of temperature in the air annulus with different thermal boundaries and water quantities.

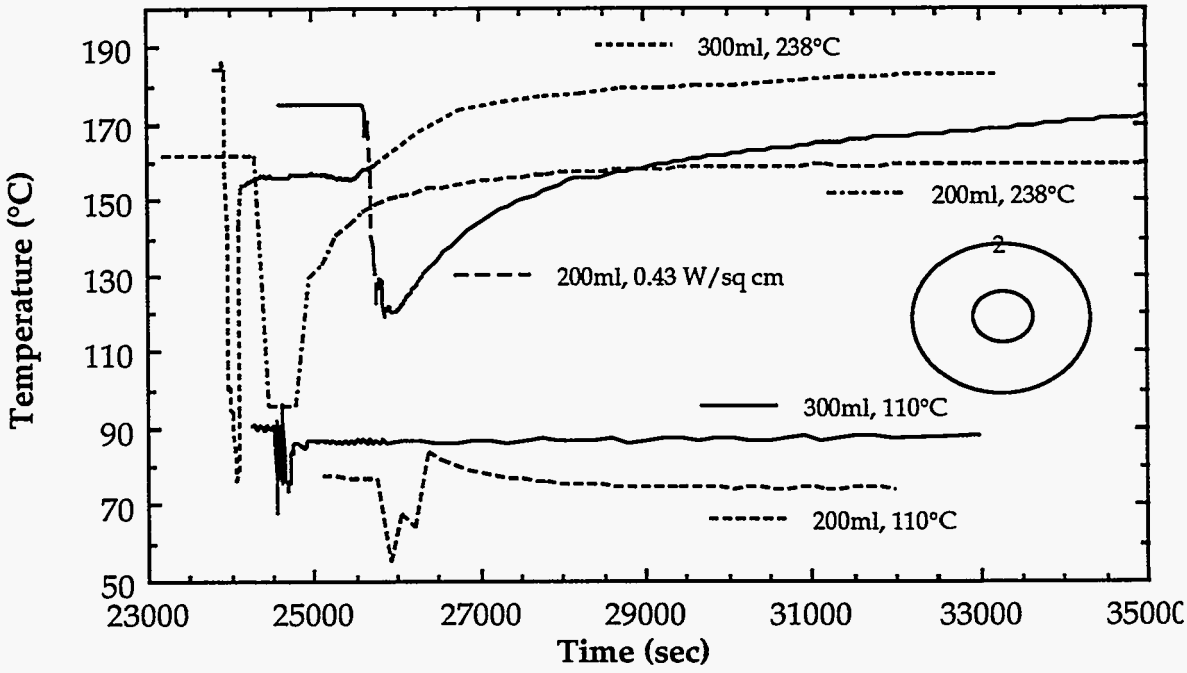

Figure 16. Comparisons of temperature in the air annulus with different thermal boundaries and water quantities.

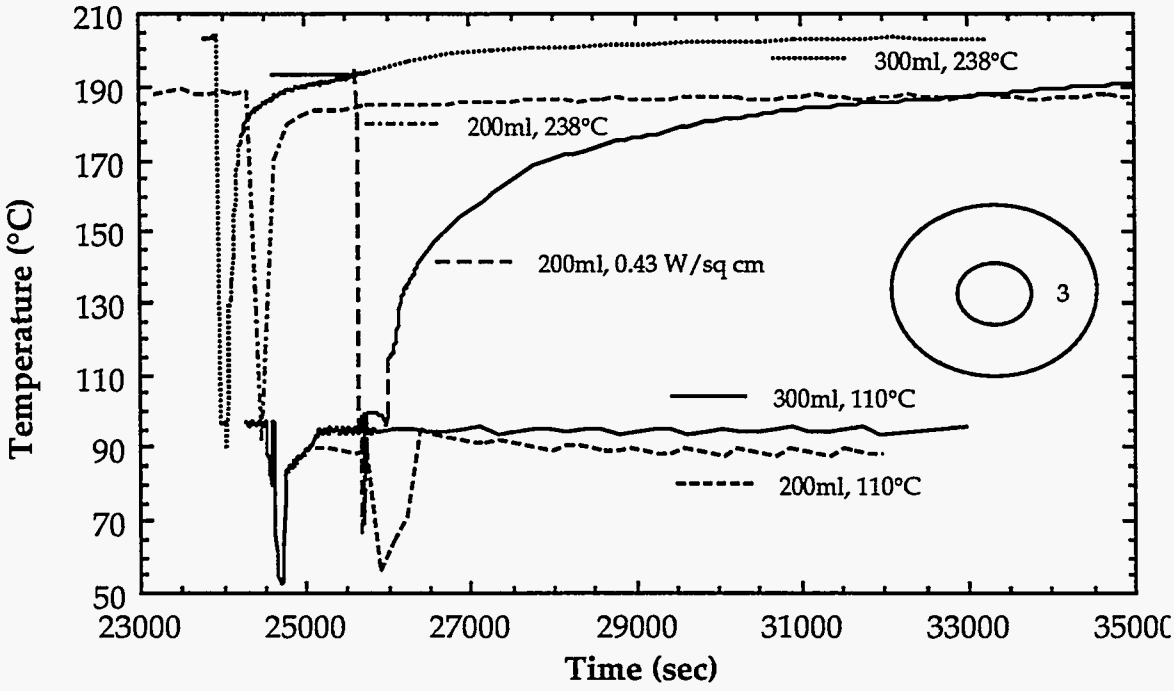

Figure 17. Comparisons of temperature in the air annulus with different thermal boundaries and water quantities.

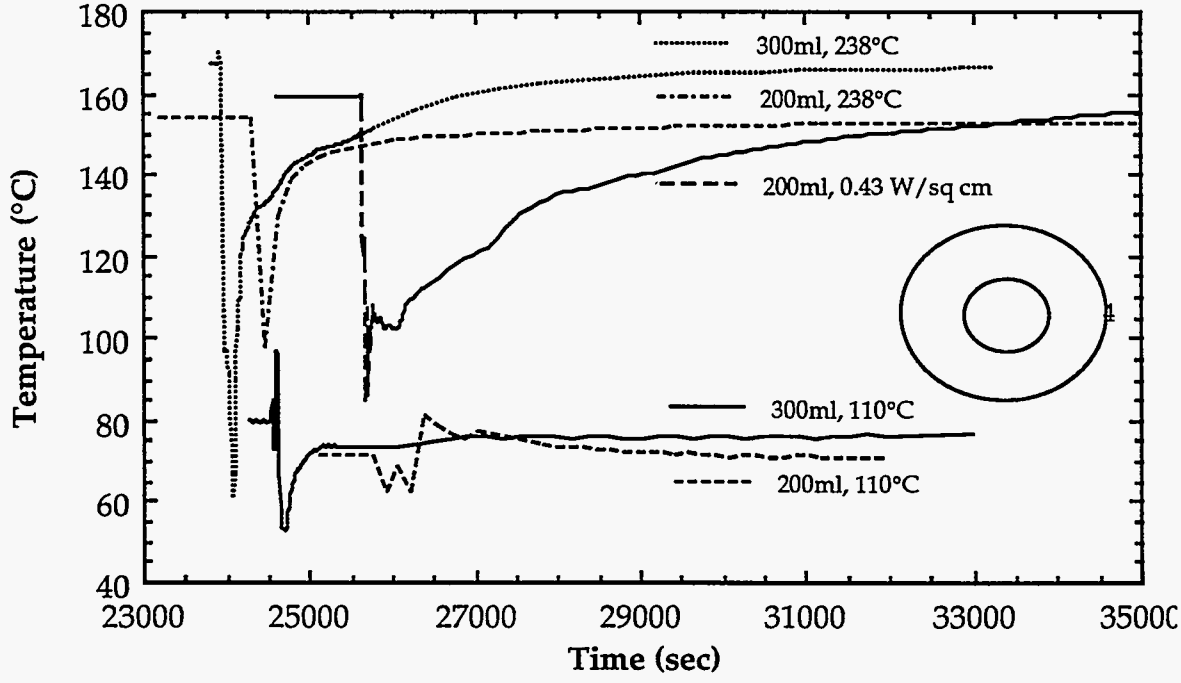

Figure 18. Comparisons of temperature in the air annulus with different thermal boundaries and water quantities.

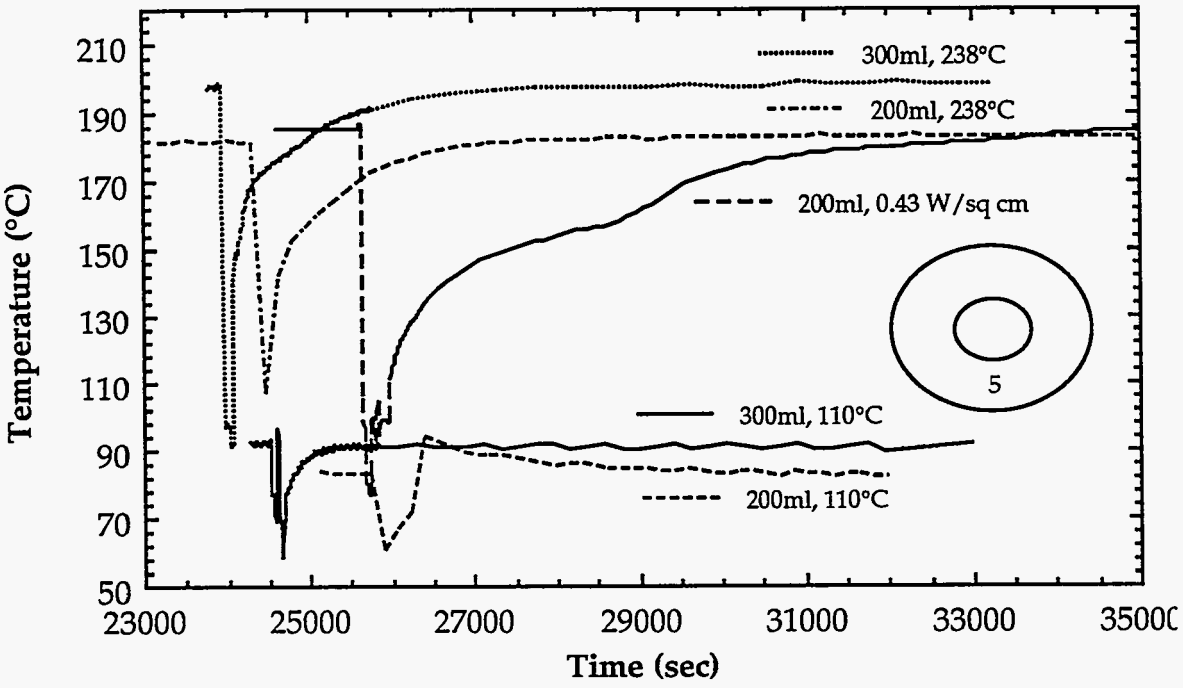

Figure 19. Comparisons of temperature in the air annulus with different thermal boundaries and water quantities.

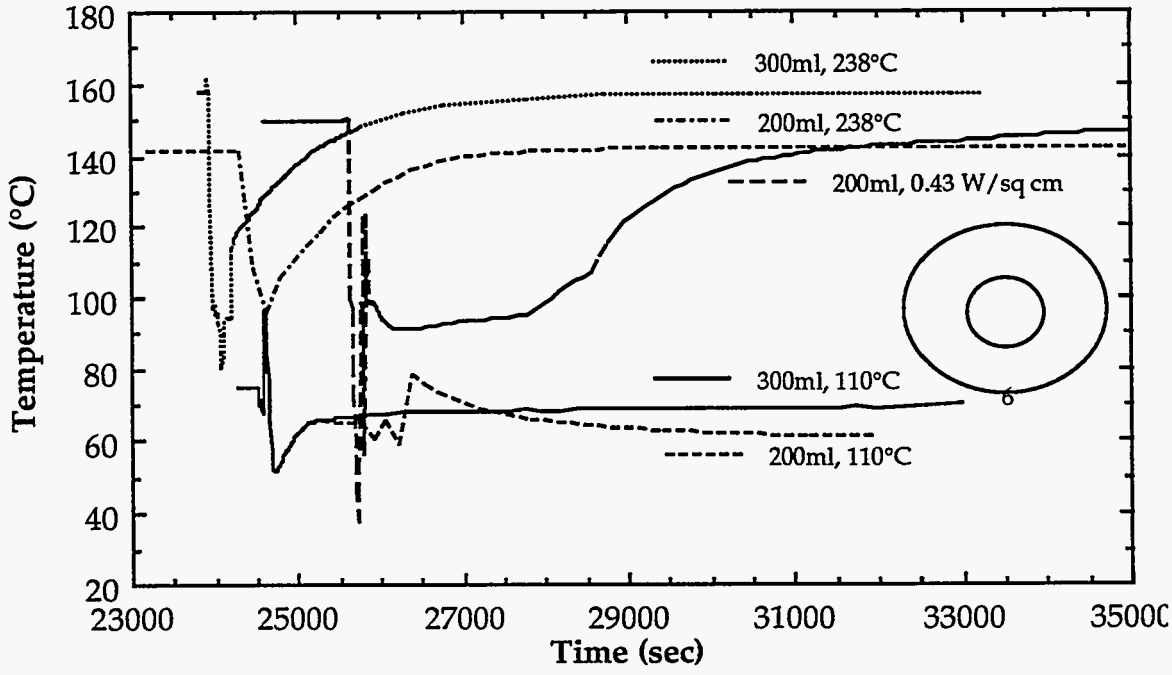

Figure 20. Comparisons of temperature in the air annulus with different thermal boundaries and water quantities.

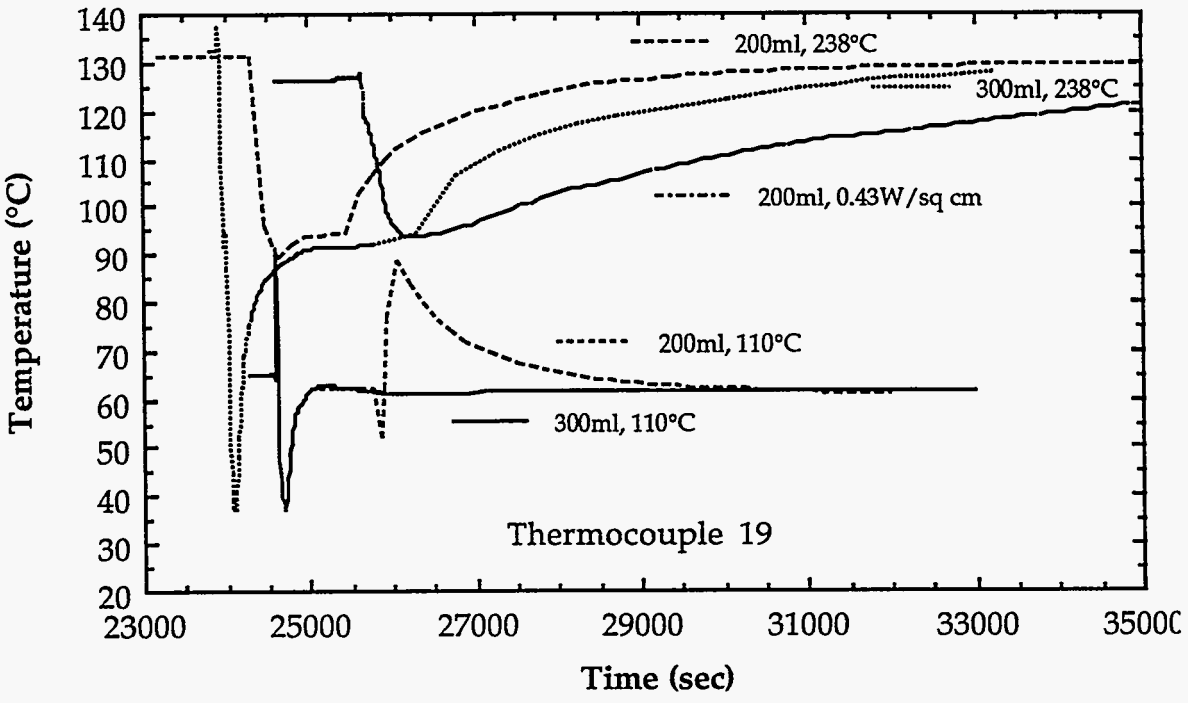

Figure 21. Comparisons of temperature in the porous medium with different thermal boundaries and water quantities.

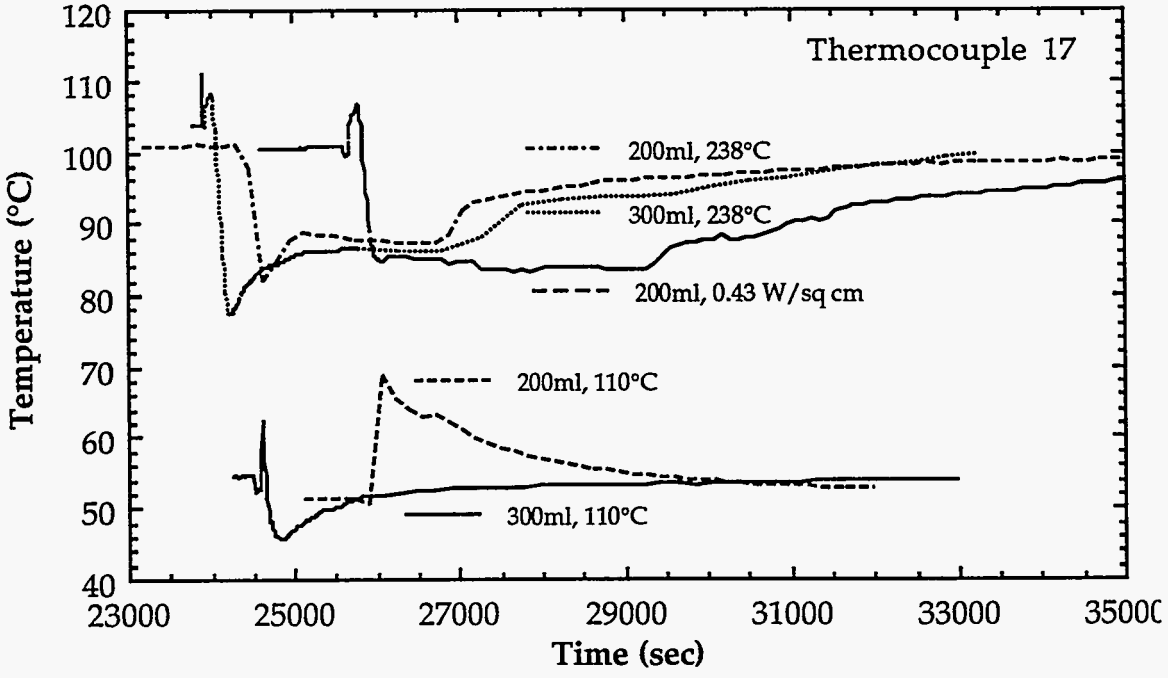

Figure 22. Comparisons of temperature in the porous medium with different thermal boundaries and water quantities.

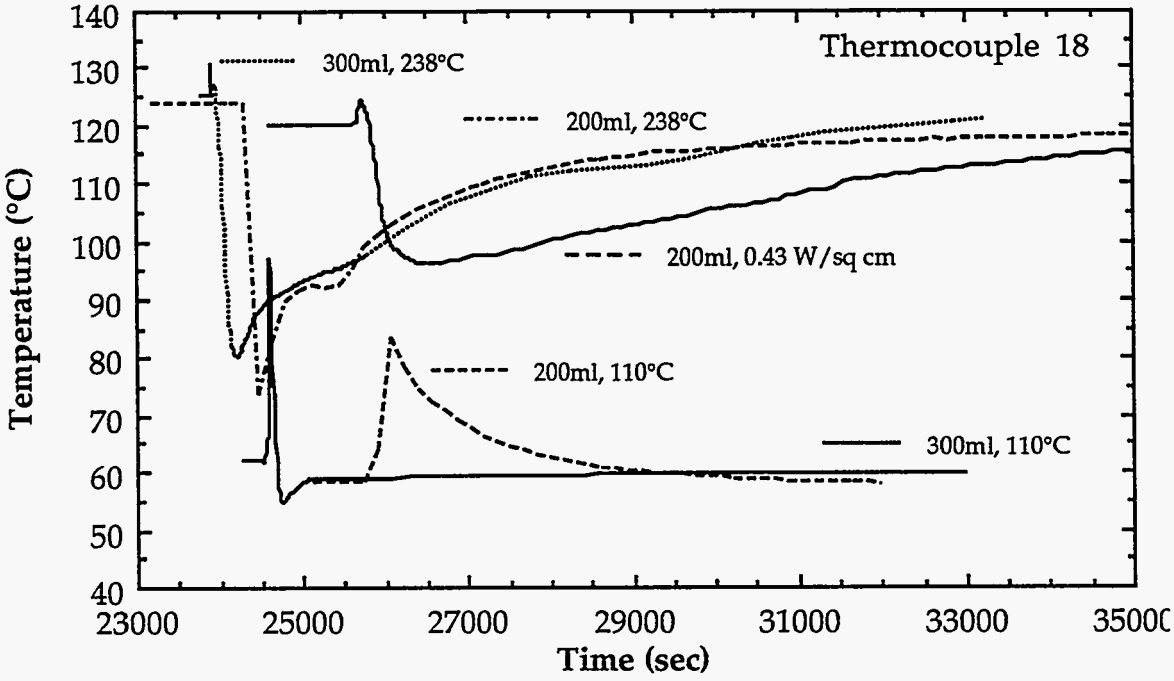

Figure 23. Comparisons of temperature in the porous medium with different thermal boundaries and water quantities.

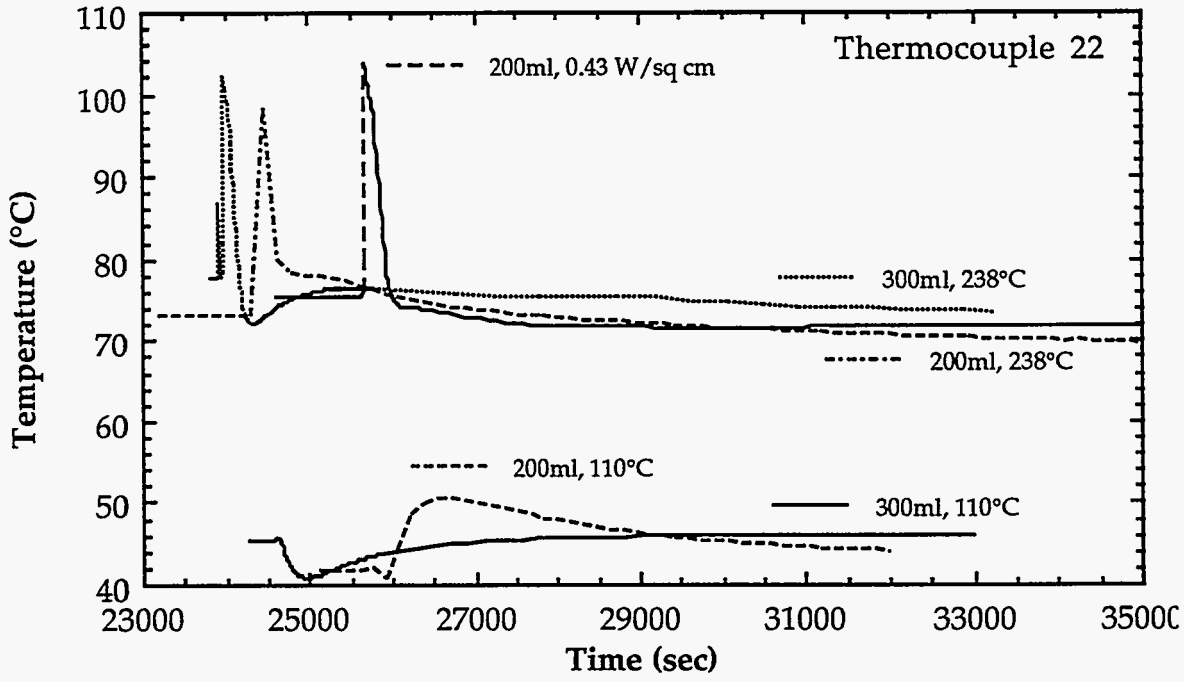

Figure 24. Comparisons of temperature in the porous medium with different thermal boundaries and water quantities.

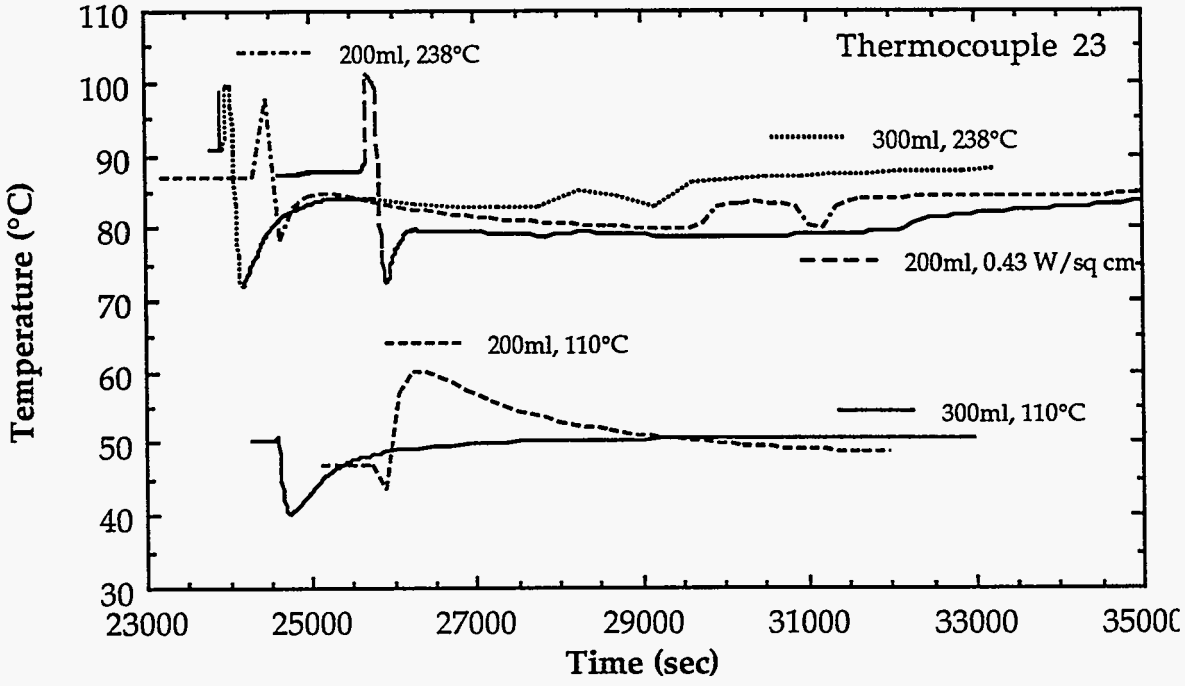

Figure 25. Comparisons of temperature in the porous medium with different thermal boundaries and water quantities.

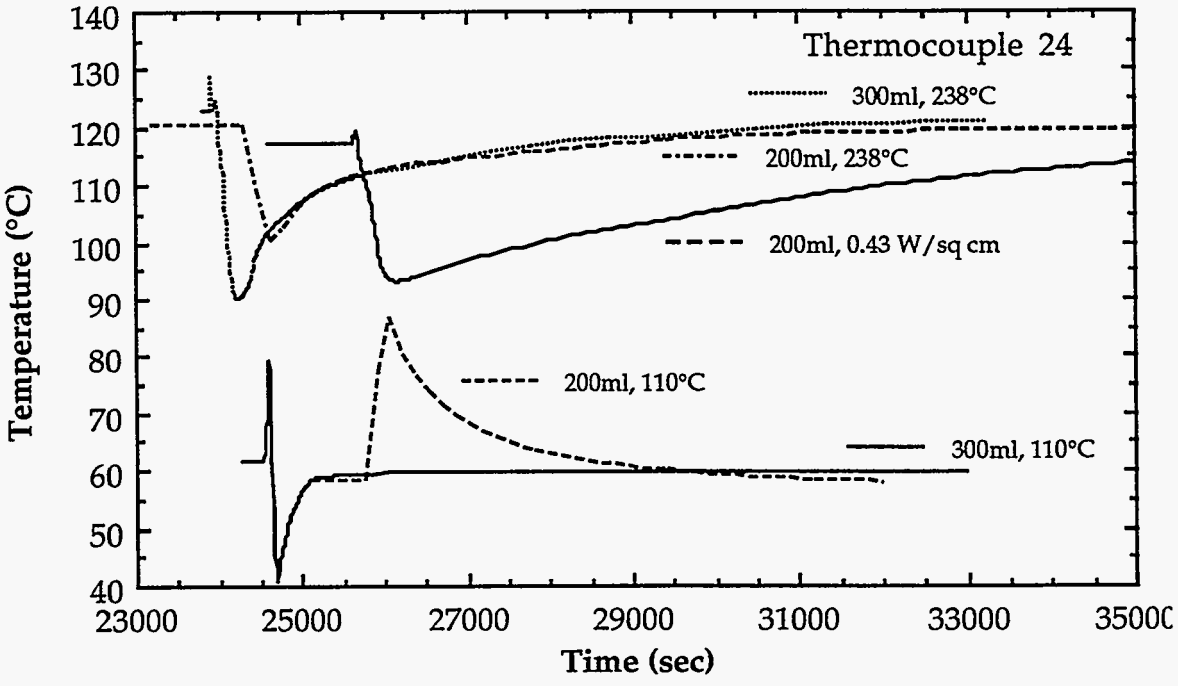

Figure 26. Comparisons of temperature in the porous medium with different thermal boundaries and water quantities.

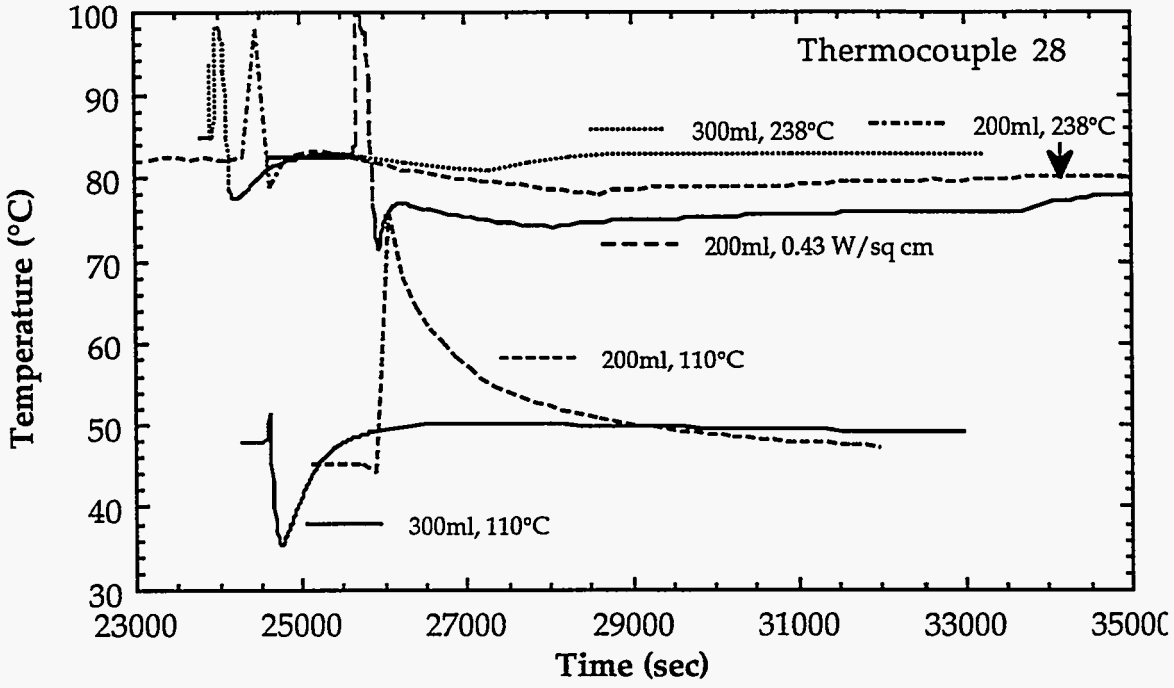

Figure 27. Comparisons of temperature in the porous medium with different thermal boundaries and water quantities.

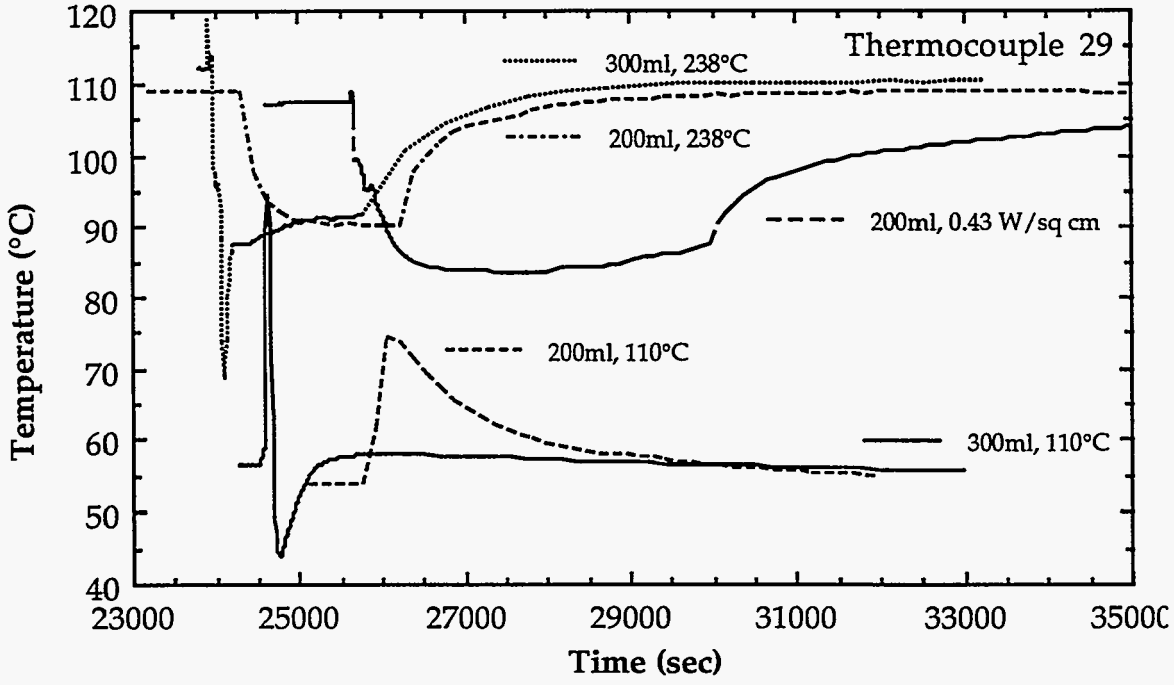

Figure 28. Comparisons of temperature in the porous medium with different thermal boundaries and water quantities.

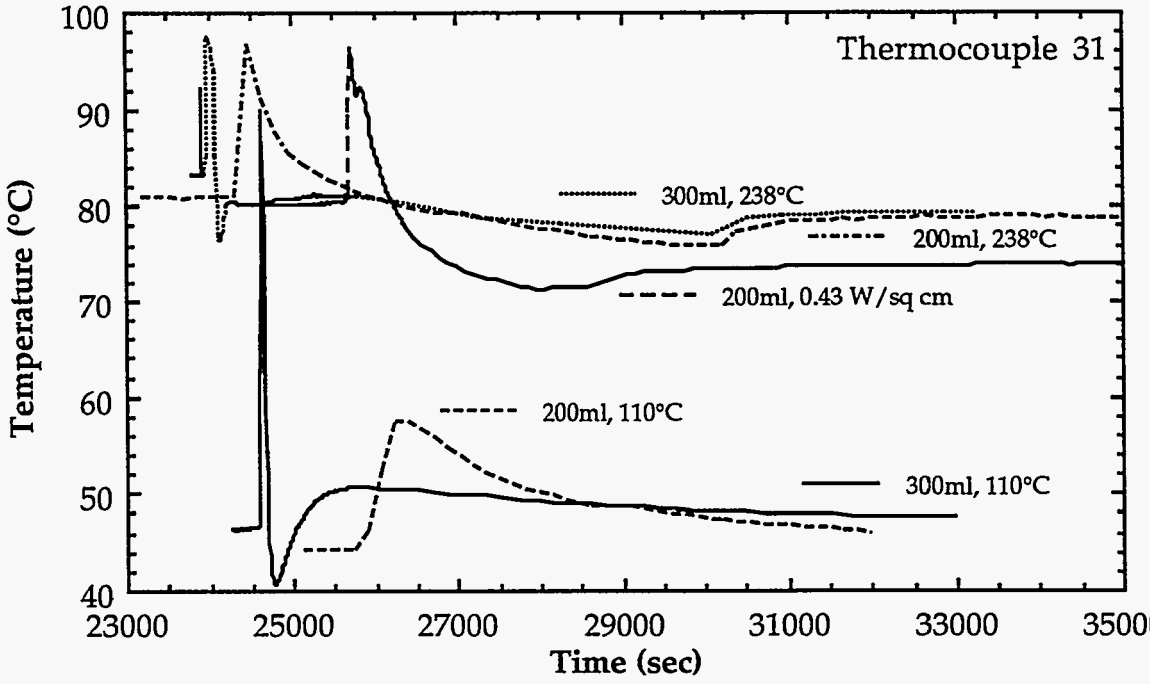

Figure 29. Comparisons of temperature in the porous medium with different thermal boundaries and water quantities.